Green Chemistry

PAPER

View Article Online
View Journal | View Issue

Cite this: *Green Chem.*, 2014, **16**, 4906

NIR provides excellent predictions of properties of biocoal from torrefaction and pyrolysis of biomass

Torbjörn A. Lestander,*[a] Magnus Rudolfsson,[a] Linda Pommer[b] and Anders Nordin[b]

Received 5th December 2013,
Accepted 1st October 2014

DOI: 10.1039/c3gc42479k

www.rsc.org/greenchem

When biomass is exposed to high temperatures in torrefaction, pyrolysis or gasification treatments, the enrichment of carbon in the remaining 'green coal' is correlated with the temperature. Various other properties, currently measured using wet chemical methods, which affect the materials' quality as a fuel, also change. The presented study investigated the possibility of using NIR spectrometry to estimate diverse variables of biomass originating from two sources (above-ground parts of reed canary grass and Norway spruce wood) carbonised at temperatures ranging from 240 to 850 °C. The results show that the spectra can provide excellent predictions of its energy, carbon, oxygen, hydrogen, ash, volatile matter and fixed carbon contents. Hence NIR spectrometry combined with multivariate calibration modeling has potential utility as a standardized method for rapidly characterising thermo-treated biomass, thus reducing requirements for more costly, laborious wet chemical analyses and consumables.

Introduction

The world's population has exceeded seven billion and the world's cumulative anthropogenic carbon dioxide (CO_2) emissions have now passed half of its first trillionth tonne.[1,2] The emission rate has risen by more than 3% annually during the last decade and despite an on-going global economic depression, CO_2 emissions reached all-time record levels in 2013.[3,4] This increases risks of the Earth's atmospheric system undergoing rapid, irreversible climatic, environmental and ecological changes.[5] Further, critical thresholds of maximum safe cumulative emissions may already have been exceeded,[5–8] although such thresholds may not be reached for some time.[9] Thus, sustainable socio-economic activity requires the rapid development (and implementation) of large-scale technological systems based on sustainable, CO_2-neutral energy sources. One such source, for both energy generation and the manufacture of diverse products, is biomass.

The transition from using mainly fossil fuels to relying more on biomass in the energy sector has been initiated. Today, renewable energy meets about 16% of total global energy demands.[10] According to recent international energy outlook published by the US Energy Information Agency renewables in general, and biomass in particular, will be among the world's fastest-growing energy sources.[11] Hence, the use of biomass in all thermal energy-yielding processes (*e.g.* combustion and co-firing) and processes as torrefaction, pyrolysis and gasification for the production of biofuels is expected to grow. For example, in the USA, generation of non-hydroelectric renewable electricity from biomass is expected to more than triple by 2035.[11]

However, in order to control torrefaction, pyrolysis and gasification process steps effectively there is a need for efficient, on-line techniques for monitoring key variables (*e.g.* H/C and O/C atomic ratios, which decline in the residual carbonized solid product when biomass is subjected to any of these processes).

Covalent C–O, C=O and C=C bonds are present in torrefied biomass, and in addition to C–H and O–H bonds their vibrations interfere with near infrared (NIR) radiation,[12] *i.e.* overtones from fundamental vibrations in the infrared (IR) region. Thus, overtone vibrations in the NIR region (having larger penetration depths than in IR) provide valuable chemical information about the state of carbonised biomass, and robust NIR instruments, which can even be used in harsh industrial environments, have been developed.

NIR techniques can be used for monitoring and controling traditional biomass refinement and conversion processes as well as the emerging torrefaction processes.[12–14] Due to their rapidity, time- and cost-effectiveness, low requirements for sample preparation and negligible use of consumables, NIR analyses have also been utilized in standardized procedures for measuring diverse variables in other kinds of biological material, *e.g.* protein contents of wholegrain wheat and seed moisture content.[15,16] It may therefore be possible to develop robust, real-time NIR-based, 'green chemistry' methods for

[a]*Swedish University of Agricultural Sciences, Department of Forest Biomaterials and Technology, SE 901 83 Umeå, Sweden. E-mail: torbjorn.lestander@slu.se; Tel: +46-907868795*
[b]*Umeå University, Department of Applied Physics and Electronics, SE 901 87 Umeå, Sweden*

characterizing torrefied biomass, biochar and solid residues after gasification, that have major advantages over traditional, wet chemistry techniques.

The main objective of this study was therefore to study the possibility of using NIR spectroscopic techniques combined with multivariate calibration modeling to predict an array of properties of torrefied biomass, biochar and the solid residue after gasifying biomass, and thus reduce the need for wet chemical analysis to characterize these 'green coals', *i.e.* carbon enriched remains after thermotreatment of biomass. Another objective was to determine if NIR spectroscopy has potential utility as an international standardized technique for assessing key variables such as the H/C and O/C atomic ratios and energy content of thermotreated biomass, especially torrefied biomass and biochar after pyrolysis.

Methods and materials

Biomass model

Biomass samples were obtained from two model species: above-ground parts of the agro-crop reed canary grass (*Phalaris arundinacea* L.), as a model for rhizomatous and energy grasses (others include *Miscanthus* ssp. and switch grass), and wood from the forest tree species Norway spruce (*Picea abies* Karst. (L.)) as a representative of woody species. In both cases, samples of both un-treated (dried to dryness) and thermal treated materials were milled over a 1 mm sieve using a laboratory mill.[17] The samples were then split into pairs of subsamples: one for wet chemical analysis to obtained reference values of the measured variables and the other for spectroscopic analysis.

Torrefied biomass. Torrefaction, or mild pyrolysis, is a promising thermal pre-treatment step prior to biomass conversion processes such as gasification and co-firing. It improves the quality of raw lignocellulosic biomass as a fuel by (*inter alia*) reducing its hydrophilicity, grinding resistance, oxygen content, inhomogeneity and bio-contamination, while raising its initially low energy content.

Torrefaction is performed by applying temperatures ranging from 200 to 340 °C in the absence of oxygen.[46] During the process the biomass is partly devolatilized, its hemicellulose and oxygen contents decrease, while its heating value increases, and other properties change.[18] Biomass samples of pelletized reed canary grass (8 mm in diameter) and chips of Norway spruce wood (typically < 4.5 × 15 × 30 mm) were torrefied at temperatures between 240 °C and 300 °C with a residence time of 8 to 25 minutes in continuos pilot-scale torrefaction facility at the Biofuel Technology Centre of the Swedish University of Agricultural Sciences in Umeå, Sweden. In all 34 torrefied samples were collected.

Biochar. Biochar samples (*ca.* 0.8 kg) were collected from 5–20 cm wood pieces of sawn and dried planks pyrolysed in a commercial plant[19] for 8–14 h and reaching at about 450 °C the two last hours. The samples may have included wood originating from Scots pine (*Pinus sylvestris* L.) besides Norway spruce. Other biochar samples (size of about 0.01–0.05 kg) were from chips of spruce stem wood treated at 350–600 °C for 4 to 40 minutes for these 16 samples.

Samples (*ca.* 0.1 kg) of the solid residue after gasification of particles (<1 mm) from reed canary grass and Norway spruce, respectively, at about 850 °C and a residential time of in average 4.0 seconds were collected from the ETC experimental plant in Piteå, Sweden.

Analysed reference variables

The energy (calorific value), ash, volatile matter and fixed carbon contents of the samples were determined according to European standard methods.[20–23] Carbon (C), hydrogen (H), oxygen (O; calculated), nitrogen (N) and sulphur (S) contents (wt%, dry basis) of samples were analysed according to a standard method.[24] Atomic H/C and O/C ratios were calculated from mass concentrations of these elements. All analysed parameters were used as reference variables in modelling. Data of mass yield expressed as the ratio (in %) of remaining dry mass of the thermo treated sample in relation to its dry mass when untreated was also recorded for most of the samples.

When concentrations of C, H, O, N, S and ash are known it is possible to predict the gross calorific value (GCV) in biomass using the following formula, developed by Gaur and Reed:[25]

$$P_{GCV} = 0.3491 \times C + 1.1783 \times H - 0.1034 \times O - 0.0151 \times N + 0.1005 \times S - 0.0211 \times \text{ash} \quad (1)$$

where P_{GCV} is the estimated gross calorific value in kJ g^{-1} and C, H, O, N, S and ash are the mass concentrations of the respective elements (in %) of dry biomass. This calculated heating value may be biased and the Pellet Handbook[26] states that this calculation overestimates GCV values by 1.8% on average.

NIR spectra and FT-IR spectroscopy

NIR spectra were collected by a Perten spectrometer[27] using a mirror cup for small sample volumes exposing about 20 cm^2 surface area (diameter: 5.06 cm). Each subsample consisted of about 11 ml, or 1.5 to 5.2 g, depending on the density of the material. Average reflectance spectra of 50 scans (during 3 seconds) at every wavelength from 950 to 1650 nm were recorded from triplicates of each milled sample and were converted into absorbance values. In total 58 × 3 spectra with 701 data points were used for modelling relationships between the spectra and measured variables (as described below).

Because of overlapping, weak peaks and broad bands of overtone vibrations in NIR also IR spectrometry was used to obtain more clear absorption peaks from fundamental molecule vibrations. FT-IR (Fourier transform infrared) reflectance spectra were collected on a Bruker IFS 66 v/S spectrometer under vacuum (400 Pa) with a standard DTGS (deuterated triglycine sulfate) detector. Manually ground KBr (infrared spectroscopy grade, Fisher Scientific, UK) was used as background. Approximately 10 mg of dry sample was mixed with

390 mg KBr and manually ground in agate mortar. A spectral resolution of 4 cm^{-1} was used and spectra from the sample-KBr blend were recorded over the region of 400–5200 cm^{-1} and 128 interferograms were co-added to obtain high signal to noise ratio. For Fourier transformation, Blackman-Harris 3-term apodization function and a zero filling factor of 2 were used and background adjusted spectra were transformed in absorbance mode.

To gain better overview spectra were grouped into classes according to the carbon content of the samples and only average spectrum for each class were shown in some figures.

Modelling and diagnostics

Principal component analysis (PCA) was used for overviewing the spectral data, and partial least squares (PLS) regression based on mean-centred NIR spectra and values of reference variables obtained for each sample, was used in the calibration modelling.[28–30] For these analyses the SIMCA 12.0,[31] Matlab[32] and PLS_Toolbox[33,34] software packages were used.

Fig. 1 shows a flow chart of how to use spectral information in the NIR region and multivariate calibration modelling to predict a range of reference values that otherwise have to be analysed by wet-chemical methods, and, how to improve modeling over time by addition of spectroscopic and reference data from new samples.

The model coefficients calculated by PLS regression modeling, *e.g.* for the prediction of GCV, are the $\boldsymbol{b}$ vector in $\boldsymbol{y} = \boldsymbol{Xb} + \boldsymbol{f}$ (here $\boldsymbol{y}$ here is the vector of observed values *e.g.* GCV, $\boldsymbol{X}$ is the matrix of NIR spectral values and $\boldsymbol{f}$ is the vector of residuals). By knowing the *b*-coefficients the values of unknown samples can be predicted *i.e.* the *y*-value for each new sample is estimated by multiplying the *b*-coefficients with the spectrum form this new sample. If the value of the unknown samples is known, *i.e.* analysed using wet chemicals according to some standardised procedure, then the model can be validated and model diagnostics can be calculated. Provided that the NIR based model has sufficient accuracy than the wet based analyses can be reduced to a minimum and predictions can be made in real time and used on-line in a process.

Diagnostic statistics to evaluate the PLS calibrations were based on the residuals ($\boldsymbol{f} = \boldsymbol{y} - \boldsymbol{y}_p$) between the vectors of observed ($\boldsymbol{y}$) and predicted values ($\boldsymbol{y}_p$) in test sets. These diagnostics were: the root mean squared error in prediction (RMSEP = $[\boldsymbol{f}^T\boldsymbol{f}J^{-1}]^{0.5}$), bias (bias = $1^T\boldsymbol{f}J^{-1}$), coefficient of multiple determination ($Q^2 = 1 - \boldsymbol{f}^T\boldsymbol{f}(\boldsymbol{y}_c^T\boldsymbol{y}_c)^{-1}$), ratio of performance to deviation (RPD = $[\boldsymbol{y}_c^T\boldsymbol{y}_cJ^{-1}]^{0.5}$RMSEP^{-1} = $[(\boldsymbol{y}_c^T\boldsymbol{y}_c)(\boldsymbol{f}^T\boldsymbol{f})^{-1}]^{-0.5}$) and range error ratio (RER = $[y_{max} - y_{min}]$RMSEP^{-1}). The scalar J here is the number of observations in the test set, $\boldsymbol{y}_c$ is the centred vector of observed values while the scalars y_{min} and y_{max} are the maximum and minimum values of the reference variable, respectively, in the test set. The scalars RMSEP and bias have the same unit as the reference variable while the others are dimensionless. The number of model components that provided the first or second local minimum of RMSEP was used in the calibration modelling. To validate the models leave-one-out (L1O) validation was used, hence each model presented consisted of a subset of models equalling the number of observations (each observation was predicted only once). In many cases the data obtained for samples treated at 850 °C were omitted because they deviated significantly in the PCA models (since no observations bridged the interval 600–850 °C). Because of the design of the experimental materials no effort was made to find detection limits for the used calibration method.

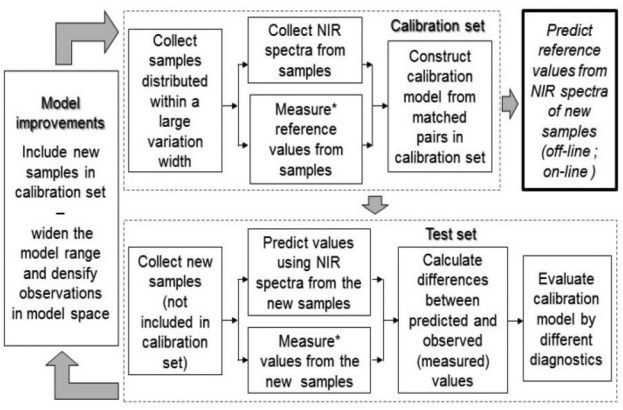

Fig. 1 Flow chart for principle of continual improvement in using spectroscopic data and calibration modelling to predict new reference values and evaluate models based on test sets (*: most often laborious wet-chemical analyses).

Results and discussion

Sample data

The carbonization treatments covered a large temperature interval, but few samples had been treated at temperatures exceeding 600 °C, thus there were few observations for modelling relationships between higher treatment temperatures and the reference variables. Table 1 presents summary statistics for the reference variables across all samples.

Table 1 Numbers of observations (obs), and mean, standard deviation (std), minimum (min) and maximum (max) values of reference variables (GCV, gross calorific value; C, carbon; H, hydrogen; O, oxygen). Units based on dry weight (d.w.)

Reference variable	# Obs	Mean	Std	Min	Max
Mass yield[a] (% d.w.)	50	62.3	28.7	19.8	100
Volatile matter[a] (% d.w.)	46	66.5	21.6	5.6	85.6
Fixed carbon[a] (% d.w.)	39	27.7	17.3	14.2	81.3
Ash (% d.w.)	58	2.9	7.2	0.2	47.7
GCV[b] (kJ g^{-1} d.w.)	58	24.9	5.1	16.8	34.0
GCV ash free[b] (kJ g^{-1} d.w.)	58	25.8	5.1	19.8	34.4
C (% d.w.)	58	63.4	14.1	47.1	90.6
H (% d.w.)	58	5.0	1.3	0.7	6.4
O (% d.w.)	58	28.3	13.6	1.5	43.1
H/C atomic ratio	58	1.01	0.40	0.17	1.50
O/C atomic ratio	58	0.38	0.22	0.023	0.66

[a] Missing values 58 minus #obs. [b] Nine values estimated by eqn (1).

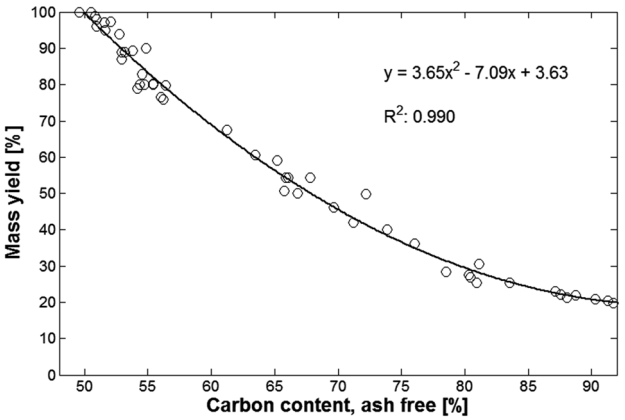

Fig. 2 Relationship between mass yield of thermotreated biomass and resulting carbon content (ash free data).

The carbon content was highest (90.6% or 95.5% on an ash-free basis) and the contents of both hydrogen and oxygen lowest (0.7% and 1.5% or as ash-free values 1.3% and 2.9%, respectively). Ash content, amount of fixed carbon and energy content increased with increasing degree of carbonisation. The atomic hydrogen to oxygen ratio also increased, indicating that relatively more oxygen was lost than hydrogen as the treatment temperature rose.

The overview also showed that there is a high correlation between carbon content and mass yield. The fitting using a 2nd order polynomial explained 99.4% of the variation, see Fig. 2.

Spectral overview

Spectral data acquired from the examined materials (Fig. 3A) clearly show that the increasing blackness (higher absorbance of radiation in visual wavelengths) of the samples caused by increasing carbonisation spills over into the NIR region. We therefore postulate that the visual region may be of interest for rough predictions of the degree of carbonisation. The change in colour of thermally modified biomass has been investigated by González-Peña and Hale[35,36] who found that colour changes are primarily linked to changes in the acid-insoluble lignin and that some colours are strongly related to specific chemical components, *e.g.* hemicellulose and lignin. For more fine-tuned predictions, information about the abundance of chemical structural groups (notably C–H, C–O and O–H) must be included in the spectral data. This information can be found in near infra-red spectra, as indicated in Fig. 3A and 3B.

Fig. 3A shows that the baseline of the NIR spectra (here, the linear regression of single spectra) shifts from a positive slope, for material treated at low temperatures, to increasingly negative slopes for material treated at higher temperatures. The absorbance at all NIR wavelengths increased with increasing treatment temperature, while the number of well-defined peaks decreased. Only 4–6% of the incident radiation from samples treated at about 850 °C was reflected to the detector. Nevertheless, first derivatives revealed that in these spectra there are still some (small) peaks at about 1400–1500 nm, indicating O–H stretching and deformation.

PCA was used to overview all NIR spectral points (in total 40 658). The first principal component (data not shown) alone was sufficient to classify the samples according to their degree of carbonization. The second principal component indicated a shift in the absorbance *versus* wavelength slope of the samples' NIR spectra at a thermal treatment temperature of around 350 °C, when the volatile matter of the remaining biochar was about 40–50%. In an analysis of nuclear magnetic resonance spectra and associated variables of torrefied wood Melkior *et al.*[37] found that depolymerisation of wood begins at temperatures of *ca.* 200 °C and increases approximately linearly as temperatures are increased to 300 °C. They also concluded that cellulose was the most stable component but after a 4 h long treatment at 300 °C Ben and Ragauskas[38] found that also cellulose in wood of loblolly pine was decomposed, and in Tang and Bacon[40] it was concluded that at 350 °C cellulose was completely decomposed. Thermogravimetric analyses of biomass thermally treated at low oxygen partial pressures have also revealed that linear breakdown of non-cellulose polymers from ~250 °C begins to end at around 350 °C.[39] Thus, the shift from positive to negative slopes indicated in the second PCA principal component (data not shown) may indicate the rapidly increasing breakdown of cellulose and lignin

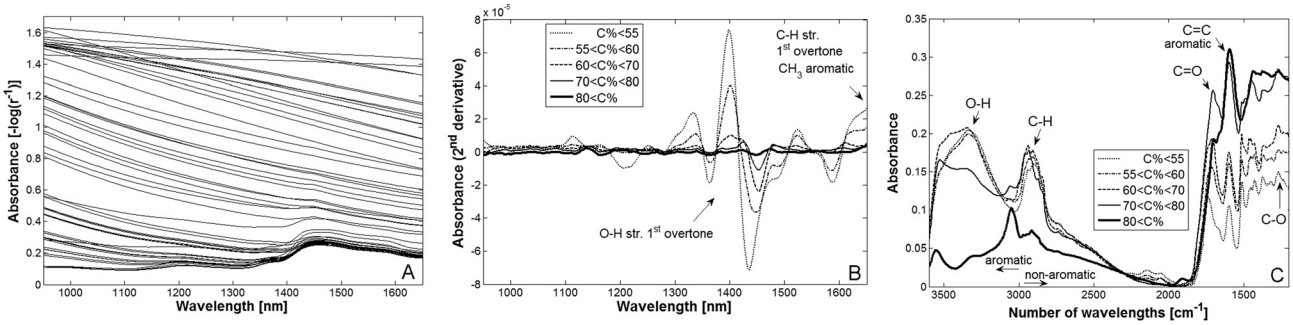

Fig. 3 A: mean NIR absorbance spectra of thermo-treated biomass at temperatures ranging from 100 to 850 °C; B and C: average of classes from <50% to >80% content of carbon (d.w.). B: NIR absorbance spectra, 2nd derivatives; C: IR absorbance spectra.

at further increases in treatment temperature followed by increased condensation of aromatic structures that results in the shift of slope.

To obtain an overview and analyse trends average of NIR and IR spectra were calculated from carbon class <55% (47.1% to 54.9%), 55–60%, 60–70%, 70–80% and >80% (80.1% to 90.6%) constituting samples ranging from 47.1 to 90.6% in carbon content (d.w.). Observations having less than 0.8% ash content were included, *i.e.* 3 samples were omitted (one observation was missing for IR carbon class 60–70%). The carbon mean value of these classes was in percent 52.4, 55.9, 65.8, 74.4 and 87.1. By using Matlab and Savitzky-Golay derivative smoothing (window size 51, polynomial of order 3 and 2nd derivative) within PLS_Toolbox 2nd derivatives that removes the influence of offset and slope were calculated for each average NIR spectrum and carbonization class (Fig. 3B). The absorbance in IR for the same classes is shown in Fig. 3C.

The 2nd derivatives of average NIR spectra showed that the higher the carbonization was the lesser derivative minima (Fig. 3B). These minima indicate where local peak values of NIR absorbance were found and the chemical assignments within Fig. 3B are according to Osborne *et al.*[41] and Shenk *et al.*[42] The average spectra of the same classes in the IR region (Fig. 3C) with chemical assignments according to Shurvell[43] showed higher absorption for the narrow bands of C=C, C=O and C–O, but lower for the broad C–H and O–H bands, when the carbonization was increased. As indicated at wavenumbers 1590–1595 cm^{-1} (C=C) and at about 3000 cm^{-1} (C–H) the aromatic component increased with degree of carbonization. Thus, in the enrichment of carbon the amount of C=C increases while going from <55 up to >80% carbon there are substantial losses of O–H and C–H. However, a proportion of O and C is successively reorganized in C–O and C=O bonds as these groups increases at higher C contents, *i.e.* when temperature was increased.

Calibration model overview

Most of the calibration models showed excellent predictive performance – especially for mass yield, volatile matter, GCV, C, O and O/C, for which RPD values exceeded 7 and, correspondingly Q^2 values exceeded 0.98 since in this case $RPD^2 = (1 - Q^2)^{-1}$ in the calibration test sets (provided that the same degree of freedom (J) is used in determination of standard deviation and RMSEP, otherwise if the degree of freedom is $J - 1$ for standard deviation then the right hand expression is multiplied by $[1 - J^{-1}]$) (Table 2). The least accurate was the ash content model based on samples with ash values from 0.2 to 1.3%, whereas nine values (all much higher than 1.3%) were excluded.

In addition to leave-one-out (L1O) modelling, we also applied ED7 tests (in which strata comprising a seventh of the data are used as test sets in each of seven runs, and each observation is predicted only once). The results were similar to those obtained by L1O modelling (data not shown) using the same number of model components and thus are not presented or further considered. This indicates that results obtained by L1O modelling do not significantly deviate from those obtained using other PLS modelling approaches. Thus, PLS modelling of data hosted in a database with numerous

Table 2 Numbers of observations (# obs), numbers of model components (A) and diagnostic statistics (RMSEP: root mean square error in prediction; Q^2: coefficient of multiple determination; RPD: ratio of performance to deviation; RER: range error ratio) of the calibration models for each of the measured variables, obtained using leave-one-out validation

Leave-one-out modelling	#Obs	A	RMSEP	Bias	Q^2	RPD[d]	RER
Non-ash free							
Mass yield (% d.w.)	50	10	3.62	−0.006	0.988	9.00	22.2
Volatile matter (% d.w.)	46	9	3.46	0.008	0.980	7.06	23.1
Fixed carbon (% d.w.)	37	10	3.28	0.330	0.966	5.46	20.1
Ash[b] (% d.w.)	49	10	0.13	−0.004	0.890	3.02	8.7
GCV[a] (kJ g^{-1})	56	14	0.75	−0.004	0.983	7.77	20.2
C[a] (% d.w.)	56	14	1.95	0.016	0.986	8.40	22.2
H[a] (% d.w.)	56	10	0.31	−0.005	0.936	3.94	12.5
O[a] (% d.w.)	56	10	1.81	0.033	0.985	8.09	21.0
H/C atomic ratio[a]	56	10	0.06	0.001	0.976	6.50	18.3
O/C atomic ratio[a]	56	10	0.03	0.001	0.988	9.33	24.0
H/C atomic ratio[a] (calculated[c])	56	—	0.06	0.001	0.976	6.46	20.5
O/C atomic ratio[a] (calculated[c])	56	—	0.02	0.001	0.988	9.28	26.9
Ash-free							
GCV (kJ g^{-1}); ash-free	58	11	1.19	−0.010	0.956	4.79	12.3
C (% d.w.), ash-free	58	12	3.30	−0.094	0.961	5.09	13.9
H (% d.w.), ash-free	58	10	0.29	0.001	0.960	5.03	17.9
O (% d.w.), ash-free	58	10	1.86	0.047	0.984	8.13	21.7
H/C (calculated[c], ash-free)	58	—	0.05	0.003	0.983	7.65	25.7
O/C (calculated[c], ash-free)	58	—	0.02	0.002	0.991	10.31	30.1

[a] The two samples from gasification was not included. [b] 9 of the ash values were not included as they regarded as outliers (≫1.3%). The mean value and standard deviation of the included (0.2–1.3%) were 0.58% and 0.34%, respectively. [c] The NIR based predictions of C, H and O, respectively, were used to calculate the ratio. [d] $RPD^2 = (1 - Q^2)^{-1}$.

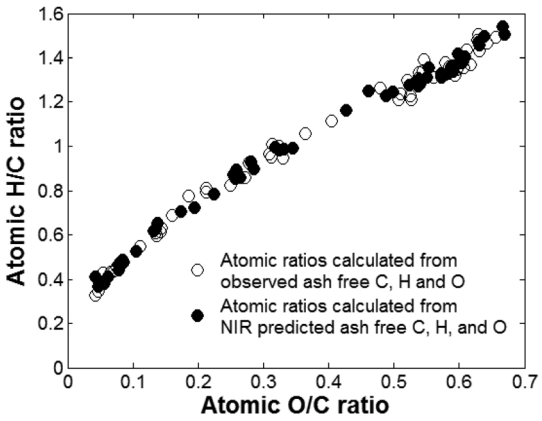

Fig. 4 Van Krevelen diagram of observed and predicted atomic H/C and O/C ratios of raw biomass and biomass treated with temperatures up to 850 °C.

observations of reference variables is likely to provide excellent predictions (*cf.* Fig. 1).

Atomic H/C and O/C ratios

The H/C and O/H atomic ratios were modelled in three ways: (i) directly by modelling each ratio and (ii–iii) indirectly by first modelling the individual C, H and O non-ash free concentrations (ii) or their ash-free concentrations (iii) and then calculating the ratios using the predicted concentrations. In the modelling the extreme observations at 850 °C were only used for ash-free models because of their large distance in ash content to other observations. The model with the highest predictive capacity is presented in Fig. 4.

Volatile matter and fixed carbon

The fixed carbon, ash and volatile matter contents are together with remaining non-ash and non-carbon (after determination of volatile matter) in total 100% of the biomass. The model for fixed carbon is not shown, but its excellent performance is indicated in Table 2. The calibration model for volatile matter obtained using L1O modelling show high accuracy, especially in the range above about 50% volatile matter. The heat treatment seemed to introduce qualitative changes influencing spectral information at around 50% of volatile matter determined by loss of material during 7 minutes at 900 °C in excess air. By splitting the data into two classes, for samples with volatile matter over and under 50% (with a few overlapping observations in both datasets to enlarge the number of observations) the predictions could be improved (data not shown).

Energy content

The calorific value of biomass is associated with the content of C, H, O, N and S and their covalent carbon bonds, and NIR spectral signals interact with most of these bonds *e.g.* C=C, C–H, C=O, C–O, O–H, N–H and S–H (except for the C–C bonds, but spectral information of C=C, C–H, C=O, C–O then provides indirect information of C–C bonds). Thus, in accordance with expectations the calibration models based on NIR spectra of both raw and thermo-treated biomass were highly accurate, as illustrated in Fig. 5A. This model explained 98.3% of the variation in GCV.

In this case too, splitting the data into two sets for two different treatment temperature ranges resulted in better performing models, with fewer components (data not shown), but doing so resulted in relatively few observations.

Fig. 5B shows the average model coefficients of the 56 PLS models and their standard deviation. It should be noted that the coefficients are calculated from mean centred data in the different calibration sets (having an all over mean value of 25.02 kJ g^{-1} for the reference variable) and the relative contribution to GCV is the product between mean centred NIR spectra and the coefficient values. This makes it difficult to interpret the model as there also are overlapping and broad bands of overtone vibrations in the NIR spectra. However, regions at about 1303 and 1454 nm showed positive

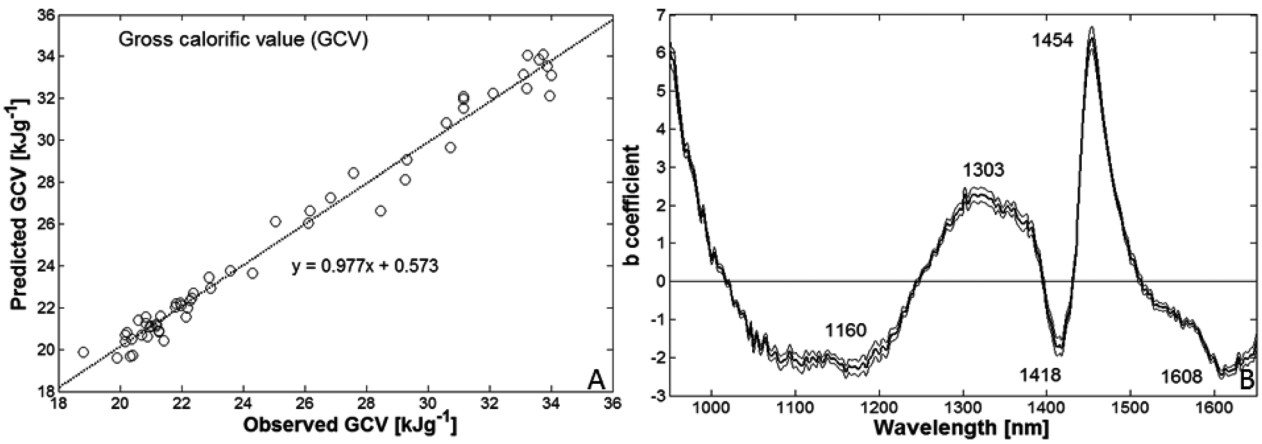

Fig. 5 A: observed and predicted energy contents (gross calorific values, GCV) of raw and thermo-treated biomass. B: model coefficients (average and ± one standard deviation) for NIR based prediction of gross calorific values.

contributions to GCV, probably associated to C–O, C═O and C═C structural groups, whereas those at 1160, 1418 and 1608 nm had most negative influence.

Another possibility, however more complicated, to estimate gross calorific value is to use only the NIR predicted contents of C, H and O and the observed ash contents *i.e.* neglecting influence of S and N as the contents these elements are low in thermotreated biomass, especially in wood. Comparison of the measured gross calorific values and those calculated from NIR predicted values using eqn (1) showed that single calculated values underestimated the energy content by in average 0.31% and the standard deviation was 19.8% of the mean observed gross calorific value (25.02 kJ g^{-1}) within the range of 18.8–34.0 kJ g^{-1} (the observations at 850 °C were not included). The linear relationship between the measured GCV and NIR calculated energy values (P_{GCV}) from C, H and O and observed ash content was $P_{GCV} = 0.9816 \times GCV + 0.5366$. The model explained 98.2% of the observed variation and the RMSEP value was about the same (0.67) as the GCV model above (see Table 2), but bias increased (−0.0766) somewhat. Thus, it is seems possible to estimate gross calorific value with high accuracy also from ash content and predicted values of C, H and O.

Conclusions

The presented results clearly show that NIR spectroscopy can be used for predicting a broad range of variables (energy, major elements in organic components, ash, volatile matter and fixed carbon contents) in the 'green coal' and biochar remaining after torrefaction, pyrolysis or gasification of biomass. Furthermore, the study indicates that NIR spectroscopy has high potential utility as a standardized technique for characterising thermo-treated biomass, and thus, reducing use of analyses based on wet chemicals. Such standards for using NIR to determine moisture and protein in whole kernels[44] but also fat, starch and crude fibers in animal feeding stuffs, cereals and milled cereal products[45] have already been implemented.

Acknowledgements

We thank: Martin Strandberg and Ingemar Olofsson at Umeå University and BioEndev for providing samples of torrefied biomass; Eleonora Borén for biochar of spruce; Rickard Gebart and Henrik Wiinikka at ETC for biochar from gasification; Håkan Örberg for samples of torrefied reed canary grass; András Gorzsás at the Vibrational Spectroscopy Platform of Umeå University for assistance with mid-infrared spectroscopic measurements and data evaluation; the Swedish national strategic Bio4Energy project, the project EU FP7 SECTOR, Processum Biorefinery Initiative, and the Swedish Energy Agency for financial support.

Notes and references

1 United Nations Population Fund, New York, USA, 2011, ISBN 978-0-89714-990-7.
2 M. R. Allen, J. David, D. J. Frame, C. Huntingford, C. D. Jones, J. A. Lowe, M. Meinshausen and N. Meinshausen, *Nature*, 2009, **458**, 1163–1166.
3 M. R. Raupach, G. Marland, P. Ciais, C. Le Quéré, J. G. Canadell, G. Klepper and C. B. Field, *Proc. Natl. Acad. Sci. U. S. A.*, 2007, **104**, 10288–10293.
4 U.S. Department of Commerce, *National Oceanic & Atmospheric Administration*, Earth System Research Laboratory, Boulder, CO, 2012, http://ftp.cmdl.noaa.gov/ccg/co2/trends/co2_annmean_mlo.txt.
5 S. Solomon, G. Plattner, R. Knutti and P. Friedlingstein, *Proc. Natl. Acad. Sci. U. S. A.*, 2009, **106**, 1704–1709.
6 W. S. Broecker, *Science*, 2007, **315**, 1371.
7 H. D. Matthews and K. Caldeira, *Geophys. Res. Lett.*, 2008, **35**, L04705.
8 M. Meinshausen, N. Meinshausen, W. Hare, S. C. B. Raper, K. Frieler, R. Knutti, D. J. Frame and M. R. Allen, *Nature*, 2009, **458**, 1158–1162.
9 J. Hansen, M. Sato, P. Kharecha, D. Beerling, R. Berner, V. Masson-Delmotte, M. Pagani, M. Raymo, D. L. Royer and J. C. Zachos, *Open Atmos. Sci. J.*, 2008, **2**, 217–231.
10 Renewables 2011 – Global status report, REN21 Secretariat Paris, France, 2011, ISSN 143792140X.
11 Annual energy outlook 2011 with projections to 2035, U.S. Department of Energy, Energy Information Administration, Office of Integrated and International Energy Analysis, Washington, DC, April 2011, http://www.eia.gov/forecasts/aeo/.
12 P. Rousset, C. Aguiar, N. Labbe and J.-M. Commandre, *Bioresour. Technol.*, 2011, **102**, 8225–8231, DOI: 10.1016/j.biortech.2011.05.093.
13 T. A. Lestander, B. Johnsson and M. Grothage, *Bioresour. Technol.*, 2009, **100**, 1589–1594.
14 T. A. Lestander and R. Samuelsson, *Energy Fuels*, 2010, **24**, 5148–5152.
15 AACC International, *Approved Methods of Analysis, 11th Ed. Method 39-25.01 Near-Infrared Reflectance Method for Protein Content in Whole-Grain Wheat*, AACC International, St. Paul, MN, USA, 2011, DOI: 10.1094/AACCIntMethod-39-25.01.
16 T. A. Lestander, R. Leardi and P. Geladi, *J. Near Infrared Spectrosc.*, 2003, **11**, 433–446.
17 Retsch, Haan, Germany.
18 D. Ciolkosz and R. Wallace, *Biofuels Bioprod. Biorefin.*, 2011, **5**, 317–329, DOI: 10.1002/bbb.275.
19 Vindelkol, Vindeln, Sweden.
20 EN 14918:2009, CEN, European Committee for Standardization, Brussels, 2009.
21 EN 14774-3:2009, CEN, European Committee for Standardization, Brussels, 2009.
22 EN 14775:2009, CEN, European Committee for Standardization, Brussels, 2009.

23 EN 15148:2009, CEN, European Committee for Standardization, Brussels, 2009.
24 EN 15104:2005, CEN, European Committee for Standardization, Brussels, 2005.
25 S. Gaur and T. B Reed, *An Atlas of Thermal Data for Biomass and Other Fuels*, NREL/TB-433-7965, UC Category:1310, DE95009212, National Renewable Energy Laboratory, Golden, Colorado, USA, 1995.
26 *The Pellet Handbook*, ed. I. Obernberger and G. Thek, Earthscan Ltd, London, 2010, ISSBN 781844076314.
27 DA 7250 NIR analyzer, Perten Instruments, Hägersten, Sweden.
28 I. T. Jolliffe, *Principal Component Analysis*, Springer, Berlin, Germany, 1986.
29 S. Wold, H. Martens and H. Wold, The multivariate calibration problem in chemistry solved by the PLS method, in *Lecture Notes in Mathematics, Proc. Conf. Matrix pencils March 1982*, ed. A. Ruhe and B. Kågström, Springer, Heidelberg, Germany, 1983, pp. 286–293.
30 H. Martens and T. Næs, *Multivariate Calibration*, John Wiley & Sons Ltd, Chichester, UK, 1989.
31 Umetrics, Umeå, Sweden.
32 The Mathworks, Inc., Natick, Mass.
33 Eigenvector Research, Manson, Wash.
34 B. M. Wise, N. B. Gallagher, R. Bro and J. M. Shaver, *PLS_Toolbox 3.0*, Eigenvector Research Inc., Manson, WA, USA, 2003.
35 M. M. González-Peña and M. D. C. Hale, *Holzforschung*, 2009, **63**, 385–393, DOI: 10.1515/HF.2009.078.
36 M. M. González-Peña and M. D. C. Hale, *Holzforschung*, 2009, **63**, 394–401, DOI: 10.1515/HF.2009.077.
37 T. Melkior, S. Jacob, G. Gerbaud, S. Hediger, L. Le Pape, L. Bonnefois and M. Bardet, *Fuel*, 2011, **92**(1), 271–280, DOI: 10.1016/j.fuel.2011.06.042.
38 H. Ben and A. J. Ragauskas, *Green Chem.*, 2012, **14**, 72–76.
39 S. Román, J. M. V. Nabais, C. Laginhas, B. Ledesma and J. F. González, *Fuel Process. Technol.*, 2012, **103**, 78–83, DOI: 10.1016/j.fuproc.2011.11.009.
40 M. M. Tang and R. Bacon, *Carbon*, 1964, **2**, 211–220.
41 B. G. Osborne, T. Fearn and P. H. Hindle, *Practical NIR spectroscopy with applications in food and beverage analysis*, Longman Scientific & Technical, Harlow, Essex, England, 2nd edn, 1993.
42 J. S. Shenk, J. J. Workman and M. O. Weterhaus, Application of NIR spectroscopy to agricultural products, in *Handbook of Near-Infrared Analysis*, ed. D. Burns and E. W. Ciurczak, Marcel Dekker, NewYork, USA, 2nd edn, 2001, pp. 419–474.
43 H. F. Shurvell, Spectra-Structure Correlations in the Mid- and Far-infrared, in *Handbook of Vibrational Spectroscopy*, ed. J. M. Chalmers and P. R. Griffiths, John Wiley & Sons, Chichester, 2001, vol. 3, pp. 1783–1816.
44 EN 15948:2012, CEN, European Committee for Standardization, Brussels, 2012.
45 ISO 12099:2010, CEN, European Committee for Standardization, Brussels, 2010.
46 A. Nordin, L. Pommer, M. Nordwaeger and I. Olofsson, Conversion of biomass through torrefaction, in *Technologies for converting biomass to useful energy, Combustion, gasification, pyrolysis, torrefaction and fermentation*, ed. E. Dahlquist, CRC Press, Leiden, The Netherlands, 2013, pp. 217–244.